Magma storage, eruptive activity and flank instability: inferences from ground deformation and gravity changes during the 1993-2000 recharging of mt. Etna volcano

Bonaccorso A., Bonforte A., Currenti G. , Del Negro C., Di Stefano A., Greco F.

Istituto Nazionale di Geofisica e Vulcanologia, Italy

Journal of Volcanology and Geothermal Research

Submitted April 2010

Revised December 2010

Accepted January 2011

Corresponding author

Alessandro Bonaccorso

Istituto Nazionale Geofisica e Vulcanologia

Sezione di Catania

Piazza Roma, 2

95123 Catania – Italy

Ph. +39.095.7165800

Fax : +39.095.7165826

Email : bonaccorso@ct.ingv.it

Abstract

A long recharging period characterized Mount Etna volcano during 1993-2000 before the main explosive-effusive 2001 and 2002-03 flank eruptions. The joint analysis of ground deformation and gravity data over the recharge period reveals that different phenomena occurred within Etna's plumbing system and clearly indicates two phases spanning 1993-1997 and 1997-2000, respectively. The first phase was characterized by magma storage and accumulation at an intermediate depth (2-6 km below sea level), which provoked an overall inflation and positive gravity changes. During the second phase, the magma started to rise and intrude at shallower levels favoring the movement of the unstable eastern flank, which accelerated its sliding toward the East. The shallower magma accumulation also caused the gas exolution, associated with increasing explosive activity at the summit craters. Negative gravity changes were detected during this phase. The gravity measurements, independently of the same result obtained by geochemical studies, suggest that only 20-30% of the magma volumes supplied in the plumbing system were then erupted. The complex dynamic of rising magma beneath Mount Etna makes ground deformation and gravity measurements complementary, being able to detect different effects of magma emplacements beneath the surface. Our results also highlight how the joint use of ground deformation and gravity observations may be crucial in identifying the nature and rate of an impending period of volcanic eruptions.

Keywords : Etna, volcano, monitoring, deformation, gravity, flank instability

1. Introduction

During recent decades, marked recharging/discharging phases have been observed at Mount (Mt) Etna (e.g. Bonaccorso, 2001; Bonaccorso and Davis, 2004). The December 1991 – March 1993 lateral eruption, which represented the most important lateral eruption in the last three centuries both in terms of duration (472 days) and volume of erupted lava (about 235 x 10^6 m^3), was preceded since 1982 by a dilatation trend measured by geodetic measurements. Bonaccorso and Davis (2004), and was accompanied by an evident deflation (Bonaccorso, 1996; Puglisi et al., 2001) that indicated a depressurizing intermediate storage zone ca. 3 km below sea level (bsl) (Bonaccorso, 1996).

After the 1991-93 effusive eruption of Mt Etna, a new long recharging phase began. The recharging phase was initially characterized by explosive manifestations from the end of 1995, when several strong lava fountain episodes occurred at summit craters. The volcanic activity took place principally at the North-East (NE) crater and preceded by about one year the resumption of activity at the South-East (SE) crater, where lasted almost continuously for the next four years. The second part of the recharging period was characterized by important events, such as the strong seismic swarms in January 1998 (Bonaccorso and Patanè, 2001) and April 2001 on the western flank, the subplinian explosion on 22 July 1998, the two sub-terminal eruptions (February-November 1999 and January 2001 eruptions) fed by the SE summit crater, and more than one hundred spectacularly explosive events of lava fountains and tephra emission from the SE summit crater during 2000-2001 (La Delfa et al., 2001; Alparone et al., 2003; Behncke and Neri, 2003; Bonaccorso, 2006), which characterized an unusual and very highly explosive period. The overall continuous recharging phase culminated with the two violent and dramatic explosive-effusive eccentric flank eruptions of July-August 2001 and October 2002 – January 2003 (e.g. Allard et al., 2006, Aloisi et al., 2006 and references therein). The 2002-03 eruption was also characterized by a lateral effusive fissure propagating in the NE sector, which also promoted a marked acceleration of the eastward sliding of the volcano's south-eastern flank (e.g. Bonaccorso et al., 2006; Bonforte et al., 2007a; 2007b; 2008; Puglisi et al., 2008). These two flank eruptions marked a significant change in the volcano dynamic regime, and the study of the 1993-2000 preparatory recharging phase has a fundamental role for a deeper comprehension of the volcano's behavior. During 1993-2000, the monitoring geophysical networks provided a multi-faceted reference data set that documented the recharging phase with considerable success. The seismicity pattern indicated a radial compression around an axial intrusion consistent with a pressurization at a depth of 6 to 15 kilometers, which triggered most of the seismicity (Patanè et al., 2003; Allard et al., 2006). Concurring with a pressurization phase, all geodetic measurements (EDM, GPS and InSar data) highlighted an overall continuous horizontal expansion of the volcano edifice from 1993 to 2001. In spite of this nearly continuous expansion, the vertical pattern showed an overall uplift during 1993-1997 followed by lowering that affected mainly the south-eastern flank during 1997-2000. The 1993-1997 period represented a net inflation of the volcano edifice and the deformation pattern pointed to a pressure source located at about 4 km bsl interpreted as an intermediate

recharging magma storage (Bonaccorso et al., 2005).

Unlike the near-constant increasing horizontal expansion but similarly to the vertical up/down trend, the gravity data showed a reversal trend characterized by increase (1994-1997) decrease (1997-1999) cycle affecting mainly the central and eastern parts of the volcano and reaching a maximum increase of about 100 μGal (Budetta et al., 1999; Carbone et al., 2003). The marked gravity changes cannot be justified by elevation changes, but could rather be due to the direct gravitational effect of magma accumulation and drainage below the volcanic pile. Significant gravity variations without ground height deformation have been reported at other volcanoes (Tiampo et al., 2004; Gottsmann et al., 2006; Hautmann et al., 2010), and thus different possible mechanisms to explain the increase/decrease gravity changes were explored.

The uniqueness of the present work is twofold: (i) for the first time on Etna, the combined deformation and gravity datasets along a middle–term period (1993-2000) are investigated, and (ii) ground deformation and gravity data are systematically compared and the cross-related information obtained from the modeled sources is discussed.

In this study for the first time we analyzed together deformation and gravity recorded during the important recharging phase occurred during 1993-2000. We highlighted that the entire recharging period can be split in two main phases (1993-1997 and 1997-2000), which are related to the action of two different main sources. We show that the first one is due to a deeper magma storage and accumulation between 2-6 km below sea level, and the second is connected to the magma migration at shallower levels. For the first time we also showed that during the second phase the vertical changes clearly showed a general subsidence of the eastern volcano edifice that marked the acceleration of the seawards motion of this unstable flank.

We discuss how these sources are related to Etna's intermediate-shallow plumbing system, the explosive and eruptive activity, and the flank instability that characterized the eastern flank.

2. Ground deformation during the recharging phase

Spanning/throughout the 1991-1993 eruption, *Bonaccorso* (1996), by inverting GPS, leveling and tilt data, modeled a depressurizing ellipsoidal source located at about 3 km bsl depth. Just after the end of the 1991-1993 eruption, *Puglisi et al.*, (2001) modeled a pressurizing point source located again at about 3 km depth, by comparing the 1993 and 1994 GPS surveys, while no deep or significant shallow magmatic source apparently acted the following year (1994-1995) by analyzing GPS data (*Bonforte and Puglisi, 2003*). InSAR data covering the same two-year period (1993-1995) led (*Lundgren, et al., 2003*) to model a pressurizing spheroidal cavity at a position very similar to the 1993-1994 GPS one. From 1996 to 1997, the inflation phase underwent an acceleration as measured by GPS surveys *(Puglisi and Bonforte,* 2004).

During the entire 1993-2000 period, EDM and GPS surveys, carried out at least yearly on the volcano, showed a continuous marked areal dilatation of the measured networks (see displacement vectors in figure 3a and 3b). This behavior was also due to the radial spreading of the edifice (*Bonaccorso, et al.*, 2005; *Bonforte and Puglisi*, 2003; *Puglisi and Bonforte*, 2004,

Puglisi et al., 2004; *Houlie, et al.*, 2006b). The GPS network is shown in Figure 1. From 1993, the GPS network on Mt Etna has been continuously improved, in order to cover a wider area and increase the spatial detail in ground deformation sampling. New benchmarks are constantly added on the volcano to improve the areal coverage and the spatial density of the network; furthermore, all new benchmarks are self-centering and some of them have been installed to replace older ones (nails), measured by tripods. The new GPS network currently consists in several sub-networks: the main inner network, covering the volcano; the external reference frame, circling it on the stable sedimentary basement; the N-S profile, above 1800 m altitude and crossing the summit area; the E-W profile, at about 1800-2000 m altitude across the southern flank; the "Ionica" network, lying over the entire eastern flank of Mt Etna below 1500 m altitude; two small networks, installed across the Pernicana fault (*Bonforte, et al.*, 2007a; *Bonforte, et al.*, 2007b; *Bonforte, et al.*, 2004; *Puglisi and Bonforte*, 2004; *Puglisi, et al.*, 2008; *Puglisi, et al.*, 2001). In this paper, we consider data coming from the main inner network (Fig. 1), from those stations having a significant historical record during the investigated period (1993-2000).

From 1993 to 2000, the areal dilatation showed a near-constant linear increasing trend which indicated a roughly continuous horizontal expansion of the volcano edifice (Fig. 2, Fig. 3a, 3b). The satellite interferometry InSar data also provided a coherent picture of the overall inflation, which characterized the volcano during 1993-2000 (Lanari et al., 1998; Lundgren et al., 2003; Neri et al., 2009).

However, a more detailed analysis of the displacement components shows that the vertical changes were characterized by an increasing/decreasing behavior. During the entire 1993-2000 expansion period, we can detect a first phase (1993-97) with vertical uplift (Fig. 3a) and a following phase (1997-2000) with a vertical lowering affecting mainly the south-eastern flank (Fig. 3b).

The geodetic measurements were focused on finding the ground deformation source acting beneath the volcano. Pressurizing sources were modeled during different periods.

The recharging phase spanning 1993-1997 represented a net inflation, not affected by significant volcanic activity at summit craters, that on the contrary occurred from 1998 to 2000. The deformation data recorded during the 1993-1997 inflation were inverted to model the pressuring intermediate storage by using analytical and numerical models with ellipsoidal pressuring source in elastic rheology that inferred a vertically elongated source with center below the summit crater area at 4 km bsl (Bonaccorso et al., 2005).

After 1997, several eruptive phenomena occurred in the summit crater area. On 22 July 1998, powerful activity took place at the central crater, with a sub-plinian paroxystic explosion; this activity produced a quick deflation of the edifice, that was detected by the tilt network. Modeling of tilt data indicated the fast depressurization of a source located at about 2-3 km bsl beneath the summit craters, i.e. shallower than the inferred pressurizing source (Bonaccorso, 2006).

In February 1999, a sub-terminal eruption started at the base of the SE summit crater and this magma output caused a slowing of the inflation rate during 1999, as revealed by the areal dilatation plot in Figure 2. After the end of this sub-terminal eruption, the volcano again began to dilate at a rate similar to that measured before 1999, and during 2000 it was characterized by an

extraordinary sequence of more than a hundred lava fountains from SE crater. A pressurizing source was modeled by *Puglisi et al.*, (2008) using GPS and DInSAR data from 2000 to 2001, located at 4 to 6 km bsl beneath the upper western flank of the volcano. *Houlie et al.*, (2006a; b) inverted GPS data spanning the entire inflating phase of the volcano, from 1994 to 2001, modeling a unique pressure source located at a depth of about 6 km bsl and representing an average of the different sources modeled by considering different shorter periods.

3. Gravity during the recharging phase

The Etna gravity network for discrete measurements consists of 71 benchmarks distributed around the volcano and covers an area of about 400 km^2 (Fig. 1). Measurements over the entire Etna gravity network are usually repeated at six month to yearly intervals, although some parts of the array are reoccupied more frequently.

We analyze the microgravity data set spanning a 6-year period (1994-2000). The data were reduced for tidal effect and for instrumental drift, and were referred to Adrano (ADR) station, since it is the least likely station to be affected by volcanically-induced gravity changes (Budetta et al., 1999).

3.1 Data

The elevation of each gravity station is not systematically monitored during the gravity surveys. Nevertheless, independent ground-deformation surveys provide enough data to evaluate Etna's vertical deformation with high detail. Using GPS data collected at stations closer to the gravity ones (Fig. 1) in the same period, gravity data were corrected for the free-air effect. We use the experimental free-air gravity gradient values, ranging between 258.7 μGal/m and 378.8 μGal/m, observed at different gravity stations of the network, to correct gravity data for height variations. Figure 4 shows several selected gravity sequences collected in different zones of the volcano compared with height variations at the closest GPS station, before and after the correction. Even if gravity normally decreases as height increases, in our case the gravity and height variations are directly space-time-correlated (i.e. gravity increases with uplift), showing an uncommon similar up-down pattern for all the considered period (Fig. 4). However, height variations are too small to significantly affect surface gravity measurements and due to the directly correlation, after the free air correction, gravity sequences exhibit an even larger amplitude.

Despite the different sampling rate with which data are normally acquired on Etna, the height corrected gravity signals show two main long-term variations involving the different sectors of the volcano. A gravity increase starting during the last months of 1995 and culminating at the end of 1996, when it reached a maximum amplitude of about 100 μGal in the stations located on the southeastern flank and on the summit of the volcano. The apparent shift in time of the positive cycle (Fig. 4), which seems to exist between data sequences from different zones, could be, at least in part, the effect of the different sampling rate. At the end of 1997, the gravity field inverted

its trend and in late-1998 reached a minimum level of about -110 μGal lower than it was in 1993, before the increase took place. The gravity changes at stations very far from the summit craters (> 15 km) remain within 20 μGal peak-to-peak during the entire period especially in the West and North flanks (Fig. 4). The seasonal effects can be considered negligible, since the selected gravity variations have been extracted from the entire data set at approximately the same time every year.
To show how the 1994-1997 (positive trend) and 1997-1999 (negative trend) gravity changes are distributed over space, the height corrected gravity data acquired at 34 gravity benchmarks from the entire Etna network were contoured over two time intervals (Fig. 5a, b). Both gravity contour maps clearly show how the positive (Fig. 5a) and negative (Fig. 5b) gravity variations, identified by the different sectors of the volcano, are distributed around the volcano with a wavelength of about 10-12 km, affecting mainly the central and eastern zones, indicating also an absence of significant gravity variations elsewhere within the gravity network.

3.2 Gravity Modeling

The data sets from the entire Etna network were separately modeled for the 1993-1997 increase and 1997-1999 decrease to infer the gravity source. In order to model the observed gravity changes, we firstly investigate if the deformation source detected by geodetic data inversion (Bonaccorso et al., 2005) could justify the increase (1993-1997) and decrease (1997-1999) in the observed gravity field. The wavelength of the microgravity observations did not support the presence of mass redistribution at the depth of the proposed ellipsoidal source (Budetta et al., 1999; Currenti et al., 2007). Both the amplitude and the extent of the observed gravity changes point to a shallower gravity source with respect to the ground deformation one. In fact, the gravity anomaly affects a much smaller area (Fig. 5) with respect to the area involved in ground deformation, suggesting that the gravity source is closer to the surface. Thus we analyzed the possible source that could produce the observed gravity changes.
The observed gravity changes and ground uplift are unusually positively correlated. Although positive gravity changes are usually thought to indicate ground subsidence, the GPS measurements revealed an overall uplift. The large gravity increase during 1993-1997 accompanied by slight height changes, could be attributed to a storage of new mass beneath the volcano. In order to evaluate the characteristics of the source that caused the observed gravity changes, we investigated four models with different source geometries: sphere, prism, cylinder, and ellipsoid. We inverted the recorded gravity changes applying a Genetic Algorithm optimization procedure, searching for the source parameters that minimize the misfit between the observed and computed gravity changes (Carbone et al., 2008). As forward model, we used the analytical solutions for all the source geometries (Singh, 1977; Clark et al., 1986; Blakely 1995) and included the topography, taking into account the altitude difference between the gravity station and the source. The results show that, despite the different geometries, all the sources can reproduce the observed anomaly with a misfit lower than 20 μGal (Table 1). As an example, we report the case of a simple spherical source located at 1820 m bsl that is able to reproduce the observed gravity

anomaly (Fig. 6). The estimated mass change is linearly related to the density contrast and the volume, with a smaller density contrast yielding a larger source radius and vice versa. Thus we avoided the ambiguity inverting only the value of the mass change obtaining a value of about 320×10^9 kg. Employing a model based on a prismatic source, we found that the observed gravity change is best explained with a source located at a depth of 2160 m bsl, with a length of 2880 m, width of 1770 m and orientation NW-SE. The calculated anomaly depends on both the density contrast $\Delta\rho$ between the source and the surrounding rocks and the thickness of the source U, thus we invert the product $U \cdot \Delta\rho$ as source parameter. The estimated mass change, 340×10^9 kg, is comparable to the previous case. Considering an elongated conduit of radius 310 m, height 3320 m and depth of the center 2480 m bsl, we model the observed anomaly with a similar misfit and estimated mass change. Finally, we applied an ellipsoidal source and the best fit to the recorded data is given for a source located at a depth of 2300 m bsl, with the major semi-axes of 1360 m and the other two semi-axes of 300 m. In this case, a density contrast of 390 kg/m^3 is necessary to justify the measured gravity change. All the geometries represent plausible sources of the observed anomaly, since potential field measurements cannot unambiguously identify the shape of the source at depth. The inferred horizontal location for all the geometries is similar to the deformation source for the same period, whereas the depth of the mass center ranges between 1800 m and 2500 m bsl. The calculations show a mass increase of about 300×10^9 kg, which yields at least a source volume of about 800×10^6 m^3 considering a density contrast of 400 kg/m^3.

During 1997-1999, the similarity in wavelength and position of the negative gravity anomaly with respect to the previous gravity increase reflects a mass decrease likely to take place within the same source. The gravity decrease can be modeled with the same source used to justify the gravity increase (Table 1), assuming the value of mass change to be opposite in sign with respect to the first period. This source produces surface displacements of a few millimeters, thus it is not well detectable by ground deformation measurements.

4. Discussion

4.1 The Etna plumbing system and the two main phases of the 1993-2000 recharging period

After the 1991-93 eruption, the ground deformation and gravity data univocally indicated that the following 1993-2000 recharging process at Mt Etna occurred in two main phases.

The first phase, from 1993 (just after the end of the eruption) to 1997, was characterized by the continuous pressurization of the feeding system of the volcano. In this interval, the ground deformation modeling infers a vertically elongated pressurizing source centered beneath the central craters area about 4 km bsl (Bonaccorso et al., 2005). Moreover, ~~we showed that~~ the positive gravity anomaly can be modeled during that period with a mass accumulation centered beneath the central craters area at about 1.5 – 2 km bsl. Both gravity data and ground deformation presented in this paper and reported by literature contribute to identify the shallow-intermediate magma plumbing system. At intermediate depth (2-6 km bsl), it is composed of a vertically

298 elongated storage volume that bounds the western side of the high-velocity body (HVB) detected
299 by seismic tomography (Patanè et al., 2003). This intermediate elongated pressurizing storage
300 provokes a wide ground deformation pattern as revealed by the terrestrial and satellite geodetic
301 measurements (Fig. 3a). Then most of the magma mass is cumulated at the shallower interface of
302 the upper limit of the HVB and is detected by the gravity changes, which consequently affected a
303 smaller/narrower area (Fig. 5a). The HVB is a large plutonic body, probably composed of frozen
304 dykes, with bottom at a depth of about 18 km as clearly revealed by seismic tomography (e.g. Hirn
305 et al., 1991; Chiarabba et al., 2000). Its estimated volume is about 3-4 times larger than the
306 volcano pile, and its accretion has recently been considered as a possible cause that destabilizes
307 the eastern flank (Allard et al., 2006). The sliding of the eastern flank has been investigated by
308 different geological and structural studies since the 90s (e.g. Lo Giudice and Rasà Rust, 1986;
309 Borgia et al., 1992; Rust and Neri, 1996), and more recently measured in detail by several
310 deformation studies (see Bonaccorso et al., 2006 and references therein). The 1993-97
311 pressurization phase was characterized by a fairly continuous increase in the gravity field and an
312 overall inflation of the volcano, with horizontal expansion and diffuse uplift. Only two GPS stations,
313 on the middle and lower eastern flank of the volcano showed subsidence, revealing a first
314 expression of an incipient seawards motion of this side of Mt Etna (Fig. 3a).
315 During the second phase, after 1997 until 2000, the volcano showed a more complex behavior.
316 Indeed, gravity data showed a progressive decrease while geodetic data continued to measure a
317 horizontal expansion as shown by the areal dilatation (Fig. 2) and GPS horizontal radial
318 displacements (Fig. 3). However, the ground deformation pattern is complicated by a general
319 subsidence of GPS stations (Fig. 3b), the reverse to the uplift previously measured, but well
320 correlated to the gravity trend (Fig. 4). This subsidence mainly affected all the stations lying on the
321 eastern side of the volcano, while stations on the western and northern stable sides showed largely
322 horizontal radial motions with less significant vertical displacements.
323
324 *4.2 Magma movement: stored and erupted volumes*
325
326 During 1994-1997, the positive gravity changes indicate a source volume of about 800 x 10^6 m^3,
327 while the extruded magma during the recharging phase and the following 2001 and 2002-2003 is
328 about 200 x 10^6 m^3 (Table 2). Therefore during the period 1993-2003, which comprises the
329 recharging plus discharging phases, there are four times more accumulating than erupted magma.
330 This geophysical result agrees fairly well with the geochemistry constraints on mass accumulation
331 and discharging. In fact, based on measured volcanic SO_2 flux, at Etna the ratio between
332 degassed magma and extruded magma was calculated at about 4 in the period 1975-1995 (Allard,
333 1997) and about 3.3 in the period 1993–2004 (Allard et al., 2006). Therefore, gravity
334 measurements independently show that only 20-30% of the magma volumes supplied and
335 cumulated in the plumbing system were then erupted. The general mechanism to explain the
336 higher quantity of degassing magma is convective ascent and recycling (e.g. Kazahaya et al.,
337 2004; Stevenson and Blake, 1998). The non-degassed magma travels up the volcanic edifice; at

shallower depth the gases are released through vesiculation process and then the denser degassed magma descends in the volcanic feeding system.

This mechanism has also been proposed at Etna to explain the predominant quantity of un-erupted degassed magma (Allard, 1997). Furthermore, Allard (1997) proposes the wide plutonic body to be the final destination for the un-erupted magma, which thus contributes to the accretion of wide plutonic roots in the basement of Etna. Following this view and in accordance with Carbone et al. (2003), since most of the estimated magma has not been erupted (70-80%), it could have been recycled by the Etna plumbing system, sinking down to a deeper level, increasing and pushing the plutonic body in the Etna's basement. However, the possible gravity effect due to this scenario would cover a greater distance than the total extent of our network and thus would be beyond the limits of detection by the gravity surveys.

The exolution of the principal gases present in Etnean magmas begins at pressures of about 100-140 MPa (~ 3 - 4 km lithostatic depth), up to 10 MPa (Spilliaert et al., 2006). During its ascending path along the feeding system of the volcano, magma passed beyond the gas exolution depth and began to further vesiculate following the above considerations. Progressive vesiculation and volatile exolution, owing to the reduction of lithostatic pressure, induces significant decreases in the bulk density of the mixture of bubbles and liquid magma (Sparks, 1978). As calculated by Corsaro and Pompilio (2004), vesiculation process of magma could reduce its density up to 25%; such a density reduction on the magma storage modeled beneath the volcano is able to produce a consistent part of the gravity decrease measured from 1997 to 1999, and promote the convective magma movements. In addition, the hypothesis proposed by Carbone et al. (2009) of the rock rarefaction due to the extension and micro-fracturing induced by flank movement has to be taken into account and could further contribute to the gravity decrease. This schematic evolution also concurs well with the volcanic activity observed at summit craters of the volcano; indeed, after 1998, stronger explosive activity took place, starting from a sub-plinian eruption at the central crater in July 1998, whose source has been modeled by Bonaccorso (2006) at about 2.5 km bsl, which is shallower than the 1993-97 deformation source and at a similar depth to the modeled gravity source. In February 1999, a sub-terminal eruption started at the base of SE Crater at 2900 m of altitude lasting ten months, and strong strombolian activity took place at Bocca Nuova crater lasting until 2000, when also a total of a hundred spectacular lava fountains took place at SE crater till June 2001. This kind of activity well testifies the strong and violent degassing of the magma stored, confirming the hypothesis of the strong vesiculation process occurring along the feeding system of the volcano.

4.3 Flank instability

As already evidenced by several studies, we usually observe a dual dynamics on Etna: a deeper one related to magma movement in the crust; a shallower one related to flank sliding. In agreement with literature, we consider that magma rises from depth along the NW border of the HVB (Patanè et al., 2003), where all pressure sources are detected (see Bonforte et al., 2008 for a review). At

those intermediate depths, magma storage produces detectable ground deformation. The mass accumulation, detected by gravity data, is located at the top of the rigid HVB at the same depth of the sub-horizontal sliding surface modeled by *Bonforte and Puglisi* (2003; 2006) by ground deformation data. In these conditions, magma movements at those depths do not produce significant mass variations, due to the very small density contrast between magma and surrounding rocks. The vertical deformation pattern suggests that the flank instability, that was affecting only the lowermost part from 1993 to 1997, extended to involve the entire unstable eastern flank of the volcano after 1997. The dip angles of the displacement vectors reported in the E-W cross section (Fig. 3b), decreasing from the central part to the eastern periphery, makes the rotational slope failure kinematics of the entire eastern flank evident. The continuous and strong inflation from 1993 to 1997 induced a radial expansion of the volcano. This expansion promoted the instability of the eastern un-buttressed flank with a consequent first seawards motion (Fig. 3a, 7a).

The seawards motion triggered a feedback process between magma uprising and gravitational sliding (Walter et al., 2005). The sliding favored an extension and depressurization on the central part of the volcano facilitating magma ascent at shallower levels filling the main conduit and producing also the first attempts of lateral intrusions as detected in 1998 (Bonaccorso and Patanè, 2001); these intrusions, in turn, produced additional stress at shallow depth favoring the instability of the un-buttressed side of the volcano (Fig. 3b, 7b). The extension of the central part of the volcano produces a negative gravity variation as consequence of the medium density decrease. Furthermore, the depressurization favors the vesiculation of the magma in the conduit producing a further density decrease.

At the shallower levels, i.e. over the upper limit of the HVB, the cumulating magma can push the shallower and more unstable eastern flank (Fig. 3b, 7b), This dynamics does not allow strong pressurization, since most of the deformation produced by magma emplacement is accommodated by the displacement of the eastern side which moves downslope, provoking an extensional zone at the top of the HVB. Such non-elastic conditions produce a detectable mass accumulation with less significant ground deformation. The opposite dynamic conditions during magma upraise beneath Mt Etna makes ground deformation and gravity measurements highly complementary, being able to detect different effects of magma emplacements beneath the surface, as evidenced by *Bonforte, et al.* (2007b) in the case of the 2002-2003 dyke emplacement.

5. Conclusion

During 1993-2000, a marked recharging phase of Mt Etna preceded the main effusive-explosive lateral eruptions of 2001 and 2002-03. The deformation and gravity patterns provide powerful indications on the magma supply and accumulation mechanisms at Etna.

Both methodologies highlight that the entire 1993-2000 inflation can be divided into two main phases showing different deep and shallow dynamics of the volcano. The first one from 1993 to 1997 was characterized by the pressurization of the deeper feeding system and magma

accumulation at 2-6 km depth. The magma storage occurred at the north-western side of the high velocity body (HVB) and also on its top, where also the decollement of the eastern flank occurs. In this period, only the lower part of the eastern flank showed a first sliding movement. The magma storage pressurization provoked both an inflation and a positive gravity change due to mass accumulation. The second period from 1997 to 2000 was characterized by the upraise of magma from the deeper source towards the surface. The magma upraise within the shallow plumbing system of the volcano was accompanied by the accelerated sliding dynamic of the eastern flank as observed by geodetic measurements. In the same period, the magma migration at shallower levels produced the gas exolution feeding the reinforced volcanic and explosive activity at summit craters. The observed decrease in gravity was consistent with this process. In agreement with previous geochemistry results, the magma volume estimated from the gravity changes during the 1993–1997 is about 3.3 - 4 times higher than the magma erupted during the 1997–2003 period. We deduce that the mass decrease measured during the second period may reasonably be imputed to vesiculation and magma recycling in the deep feeding system.

A novelty revealed by the combined analysis of ground deformation and gravity data over the long inflating period from 1993 to 2000 is the correlation among the change in the kinematics of the eastern flank of the volcano, the gravity variations, the vertical motions and the eruptive activity.

In this paper, an effort was made in order to give an overall picture of the deep and shallow phenomena occurring beneath Mt Etna through ground and gravity observations. Despite the difficulties in interpreting these data jointly, the results are encouraging since the complementarity of these two approaches helps to better understand some mechanisms that precede and accompany volcanic eruptions, crucial to minimize their hazard.

References

Allard, P., 1997. Endogenous magma degassing and storage at Mount Etna, Geophys. Res. Lett., 24, 2219–2222.

Allard, P., Behncke, B., D'Amico, S., Neri, M., Gambino, S., 2006. Mount Etna 1993–2005: Anatomy of an evolving eruptive cycle, Earth Sci. Rev. 78, 85–114.

Aloisi, M., Bonaccorso, A., Gambino, S., 2006. Imaging composite dike propagation (Etna 2002, case), *J. Geophys. Res*., 111, B06404, doi:10.1029/2005JB003908.

Alparone, S., Andronico, D., Lodato, L., Sgroi, T., 2003. Relationship between tremor and volcanic activity during the Southeast Crater eruption on Mount Etna in early 2000, J. Geophys. Res. 108, 2241. doi:10.1029/2002JB001866.

Blakely, R.J., 1995. Potential Theory in Gravity and Magnetic Applications, Cambridge University Press, New York, 1995.

Behncke, B., Neri, M., 2003. Cycles and trends in the recent eruptive behaviour of Mount Etna (Italy), Canadian J. Earth Sci. 40, 1405-1411, doi: 10.1139/E03-052.

Bonaccorso, A., 1996. Dynamic inversion of ground deformation data for modelling volcanic sources (Etna 1991-93), Geophysical Research Letters, 23, 451-454.

458 Bonaccorso, A., 2001, Mt Etna volcano : modelling of ground deformation patterns of recent eruptions and
459 considerations on the associated precursors, *Journal of Volcanology and Geothermal Research*, 109, 99-
460 108, 2001.
461 Bonaccorso, A., 2006. Explosive activity at Mt. Etna summit craters and source modeling by using high
462 precision continuous tilt. Journal of Volcanology and Geothermal Research, 221-234, 158,
463 doi:10.1016/j.jvolgeores.2006.05.007
464 Bonaccorso, A., Patanè, D., 2001. Shear response to an intrusive episode at Mt Etna volcano (January
465 1998) inferred through seismic and tilt data, Tectonophysics, 334, 61-75.
466 Bonaccorso, A., Davis, P.M., 2004. Modeling of ground deformation associated with recent lateral eruptions:
467 Mechanics of magma ascent and intermediate storage at Mt.Etna, in *Etna Volcano Laboratory,*
468 *Geophys. Monogr. Ser., vol. 143*, Eds A. Bonaccorso, S. Calvari, M. Coltelli, C. Del Negro and S.
469 Falsaperla, pp. 293-306, AGU, Washington, D. C.
470 Bonaccorso, A., Cianetti, S., Giunchi, C., Trasatti, E., Bonafede, M., Boschi, E., 2005. Analytical and 3-D
471 numerical modelling of Mt. Etna (Italy) volcano inflation, *Geophys. J. Int.*, *163*, 852–862, doi:
472 10.1111/j.1365-246X.2005.02777.x
473 Bonaccorso, A., Bonforte, A., Guglielmino, F., Palano, M., Puglisi, G., 2006. Composite ground deformation
474 pattern forerunning the 2004–2005 Mount Etna eruption, *J. Geophys. Res.,111*, B12,
475 doi:10.1029/2005JB004206.
476 Bonforte, A., Puglisi, G., 2003. Magma uprising and flank dynamics on Mount Etna volcano, studied using
477 GPS data (1994-1995), Journal of Geophysical Research-Solid Earth, 108, B3,
478 doi:10.1029/2002jb001845.
479 Bonforte, A., Puglisi G., 2006. Dynamics of the eastern flank of Mt Etna volcano (Italy) investigated by a
480 dense GPS network, *Journal of Volcanology and Geothermal Research*, *153*, 357-369, doi:
481 10.1016/j.jvolgeores.2005.12.005.
482 Bonforte, A., Bonaccorso A., Guglielmino F., Palano M., Puglisi G., 2008. Feeding system and magma
483 storage beneath Mt Etna as revealed by recent inflation/deflation cycles, Journal of Geophysical
484 Research-Solid Earth, 113, B05456, doi:10.1029./2007JB005334
485 Bonforte, A., Branca, S., Palano, M., 2007a. Geometric and kinematic variations along the active Pernicana
486 fault: Implication for the dynamics of Mount Etna NE flank (Italy), Journal of Volcanology and Geothermal
487 Research, 160, 210-222, doi:10.1016/j.jvolgeores.2006.08.009.
488 Bonforte, A., Carbone, D., Greco, F., Palano, M., 2007b. Intrusive mechanism of the 2002 NE-rift eruption at
489 Mt Etna (Italy) modelled using GPS and gravity data. Geophys. J. Int., 169, 339–347, doi: 10.1111/j.1365-
490 246X.2006.03249.x.
491 Bonforte, A., Guglielmino, F., Palano, M., Puglisi, G., 2004. A syn-eruptive ground deformation episode
492 measured by GPS, during the 2001 eruption on the upper southern flank of Mt Etna, Bulletin of
493 Volcanology, 66, 336-341, doi: 10.1007/s00445-003-0314-x
494 Borgia, A., Ferrari, L., Pasquarè., G., 1992. Importance of gravitational spreading in the tectonic and volcanic
495 evolution of Mount Etna. Nature 357: 231-235.
496 Budetta G., Carbone, D., Greco, F., 1999. Subsurface mass redistributions at Mount Etna (Italy) during the
497 1995-96 explosive activity detected by microgravity studies. Geoph. J. Int., 138, 77-88.
498 Carbone, D., Budetta, G., Greco F., 2003. Possible mechanisms of magma redistribution under Mt Etna
499 during the 1994–1999 period detected through microgravity measurements. Geoph. J. Int., 152, 1–14.

Carbone, D., Currenti, G., Del Negro, C., 2008. Multi-objective genetic algorithm inversion of ground deformation and gravity changes spanning the 1981 eruption of Etna volcano. J. Geophys. Res., 113, B07406, doi:10.1029/2006JB004917.

Carbone, D., D'Amico, S., Musumeci, C., Greco, F., 2009. Comparison between the 1994 2006 seismic and gravity data from Mt Etna: new insight into the long-term behavior of a complex volcano. Earth Planet. Sci. Lett. 279, 282292.

Chiarabba, C., Amato, A., Boschi, E., Barberi, F., 2000. Recent seismicity and tomographic modeling of the Mount Etna plumbing system, J. Geophys. Res. 105, 10923-10938.

Clark, D.A., Saul, S.J., Emerson, D.W., 1986. Magnetic and gravity anomalies of a triaxial ellipsoid. Exploration Geophysics 17, 189-200.

Coltelli M., Proietti, C., Branca, S., Marsella, M., Andronico, D., Lodato, L., 2007. Analysis of the 2001 lava flow eruption of Mt. Etna from three-dimensional mapping, J. Geophys. Res., 112, F02029, doi:10.1029/2006JF000598.

Corsaro, R.A., Pompilio, M., 2004. Buoyancy-controlled eruption of magmas at Mt Etna, Terra Nova 16, 16-22.

Currenti, G., Del Negro, C., Ganci, G., 2007. Modelling of ground deformation and gravity fields using finite element method: an application to Etna volcano, Geophysical Journal International, 169, 775-786.

Gottsmann, J., Wooller, L.K., Marti, J., Fernandez, J., Camacho, A.G., Gonzalez, P., Garcia, A., Rymer, H., 2006. New evidence for the reactivation of Teide Volcano. Geophys. Res. Lett. 33. doi:10.1029/2006GL027523.

Hautmann, S., Gottsmann J., Camacho A.G., Fournier N., Sacks I.S., Stephen R. , Sparks, J., 2010. Mass variations in response to magmatic stress changes at Soufrire Hills Volcano, Montserrat (W.I.): Insights from 4-D gravity data. Earth and Planetary Science Letters, 290 (2010) 8389.

Hirn, A., Nercessian, A., Sapin, M., Ferrucci, F., Wittlinger, G., 1991. Seismic heterogeneity of Mt Etna: structure and activity, Geophys. J. Int., 105, 139–153.

Houlie, N., Briole, P., Bonforte, A., Puglisi, G., 2006a. Large scale ground deformation of Etna observed by GPS between 1994 and 2001, Geophysical Research Letters, 33, 2, L02309, doi: 10.1029/2005gl024414.

Houlie, N., Briole, P., Bonforte, A., Puglisi, G., 2006b. Large scale ground deformation of Etna observed by GPS between 1994 and 2001 (vol 33, art no L02309, 2006), Geophysical Research Letters, 33, 20, L20309, doi: 10.1029/2006gl026892.

Kazahaya, K., Shinohara, H., Uto, K., Odai, M., Nakahori, Y., Mori, H., Iino, H., Miyashita, M., Hirabayashi, J. 2004. Gigantic SO_2 emission from Miyakejima volcano, Japan, caused by caldera collapse, Geology, 32, 425-428, doi: 10.1130/G20399.1.

La Delfa, S., Patane', G., Clocchiatti, R. Joron, J.L., Tanguy J.C., 2001. Activity of Mount Etna preceding the February 1999 fissure eruption: inferred mechanism from seismological and geochemical data, J. Volc. Geotherm. Res., 105, 121–139.

Lanari, R., Lundgren, P., Sansosti, E., 1998. Dynamic deformation of Etna volcano observed by satellite radar interferometry, Geophys. Res. Lett., 25, 1541–1544.

Lo Giudice, E., Rasa', R., 1986. The role of the NNW structural trend in the recent geodynamic evolution of North-Eastern Sicily and its volcanic implications in the Etnean area, J. Geodyn., 5, 309–330.

Lundgren, P., Berardino, P., Coltelli, M., Fornaro, G., Lanari, R., Puglisi, G., Sansosti, E., Tesauro, M., 2003. Coupled magma chamber inflation and sector collapse slip observed with synthetic aperture radar interferometry on Mt Etna volcano, Journal of Geophysical Research-Solid Earth, 108, B5, doi: 10.1029/2001jb000657.

544 Neri, M., Casu, F., Acocella, V., Solaro, G., Pepe, S., Berardino, P., Sansosti, E., Caltabiano, T., Lundgren,
545 P., Lanari, R., 2009. Deformation and eruptions at Mt. Etna (Italy): A lesson from 15 years of
546 observations, Geophys. Res. Lett., 36, L02309, doi:10.1029/2008GL036151
547 Patanè, D.,De Gori, P., Chiarabba, C., Bonaccorso, A., 2003. Magma ascent and the pressurization of
548 Mount Etna's volcanic system, Science, 299, 2061-2063.
549 Puglisi, G., Bonforte, A., 2004. Dynamics of Mount Etna Volcano inferred from static and kinematic GPS
550 measurements, Journal of Geophysical Research-Solid Earth, 109, B11, doi:10.1029/2003jb002878.
551 Puglisi, G., Bonforte, A., Maugeri, S.R., 2001. Ground deformation patterns on Mount Etna, 1992 to 1994,
552 inferred from GPS data, Bulletin of Volcanology, 62, 371-384.
553 Puglisi, G., Briole, P., Bonforte, A., 2004. Twelve years of ground deformation studies on Mt. Etna volcano
554 based on GPS surveys, in *Etna Volcano Laboratory, Geophys. Monogr. Ser., vol. 143*, Eds A.
555 Bonaccorso, S. Calvari, M. Coltelli, C. Del Negro and S. Falsaperla, pp. 321-341, AGU, Washington,
556 D.C.
557 Puglisi, G., Bonforte, A., Ferretti, A., Guglielmino, F., Palano, M., Prati, C., 2008. Dynamics of Mount Etna
558 before, during, and after the July-August 2001 eruption inferred from GPS and differential synthetic
559 aperture radar interferometry data, Journal of Geophysical Research-Solid Earth, 113, B06405,
560 doi:10.1029/2006jb004811
561 Rust, D., Neri, M., 1996. The boundaries of large-scale collapse on the flanks of Mount Etna, Sicily, in
562 *Volcano instability on the Earth and other planets, Geol. Soc. Spec. Publ. 110*, edited by W. J.
563 McGuire, A. P. Jones, and J. Neuberg, 193-208.
564 Singh, S. K., Gravitational attraction of a vertical right circular cylinder, Geophys. J. R. Astron. Soc., 50, 243-
565 246, 1977.
566 Sparks, R.S.J., 1978. The dynamics of bubble formation and growth in magmas: a review and analysis, J.
567 Volcanol. Geotherm. Res. 3, 1–37.
568 Spilliaert, S., Metrich, N., Allard, P., 2006. S-Cl-F degassing pattern of water-rich alkali basalt: Modelling and
569 relationship with eruption styles on Mount Etna volcano. Earth Planetary Science Letters, 248, 772-786.
570 Stevenson, D., Blake, S., 1998. Modelling the dynamics and thermodynamics of volcanic degassing, *Bulletin*
571 *of Volcanology* , 60, 307–317
572 Tiampo, K.F., Fernandez, J., Jentsch, G., Charco, M., Rundle, J.B., 2004. New results at Mayon, Philippines,
573 from a joint inversion of gravity and deformation measurements. Pure Appl. Geophys. 161, 14331452.
574 Walter, T.R., Acocella, V., Neri, M., Amelung, F., 2005. Feedback processes between magmatic events and
575 flank movement at Mount Etna (Italy) during the 2002–2003 eruption, *J. Geophys. Res.*, 110, B10205,
576 doi:10.1029/2005JB003688
577
578
579 **Acknowledgements**
580 This study was undertaken with financial support from the V3-LAVA and V4-FLANK projects (DPC-INGV
581 2007-2009 contract). Thanks are due to A.G. Camacho and R. del Potro for their revisions and improvement
582 of the early version of the manuscript. Special thanks to B. Puglisi and the UFDG and UFGM staff of INGV-
583 CT that carries out ground deformation and gravity measurements.
584

Captions

Figure 1. Map showing the position of the height corrected gravity benchmarks of Etna's microgravity network (red triangles) and the GPS benchmarks (black circles). Dashed line contours the seawards moving flank of the volcano. The inset at the top left shows the location of Etna volcano with respect to Sicily, the one at the bottom left shows the position of the four Summit Craters (NEC = Northeast Crater, VOR = Voragine, BNC = Bocca Nuova, SEC = Southeast Crater). The benchmarks are grouped in different areas (shaded green squares numbered from 1 to 6; 1 North Zone, 2 North East Zone, 3 South East Zone, 4 South West Zone, 5 West Zone and 6 Summit Zone). The signals of the labeled gravity and GPS benchmarks within each zone are presented in Figure 4. Geographical coordinates are expressed in UTM projection, zone 33N.

Figure 2. Cumulative areal dilatation calculated since 1990 for the area covered by the GPS network.

Figure 3. Map and section of the displacements measured in the intervals 1993-1997 (a) and 1997-2000 (b), respectively. The area within the dashed white square is covered by the gravity contour maps shown in Figure 5a, b.

Figure 4. Selected gravity signals collected in different areas (labeled in Figure 1) of the volcano from 1993 to 2000 compared with height variations at the closest GPS station, before and after the free air correction.

Figure 5. Sketch maps showing gravity changes for the (A) July 1994 – June 1997 (gravity increase) and (B) June 1997 – June 1999 (gravity decrease) periods.

Figure 6. Gravity changes expected from a spherical source located under crater area at 1820 bsl (A). Different geometries can reproduce a similar pattern (see Table 1 for the complete parameters of the sources). Map of the residual gravity values from the model (B).

Figure 7. Sketch map of the main phases during the 1993-2000 recharging. Magma rises from the deeper levels (1) along the western border of the high velocity body (HVB). At intermediate depth of about 4 km bsl, the magma is stored in a vertically elongated source (2) located in the upper western border of the HVB as inferred by ground deformation modeling. The pressurization of this source provokes a near-continuous expansion of the volcano edifice. (A) During 1993-1997, magma is also accumulated along the upper limit of the VHD (3) as inferred by the gravity changes pattern. In this period, a first sliding toward the East was recorded in the lowermost part of eastern flank through sliding planes modeled in previous studies (see references in the text). (B) During 1997-2000 the gases are released, a high explosivity characterized this period; then the denser degassed magma descended in the volcanic feeding system provoking a gravity decrease.

Table 1 - Source parameters inferred from inversion of gravity data.

Table 2 - Magma erupted volumes during the period 1993-2004 after Behncke and Neri (2003), Allard et al. (2006) and Coltelli et al. (2007). The estimated volumes take into account both lava (emitted from effusive eruptions, lava flows from eruptive episodes and overflows from central craters) and tephra (emitted from explosive activity).

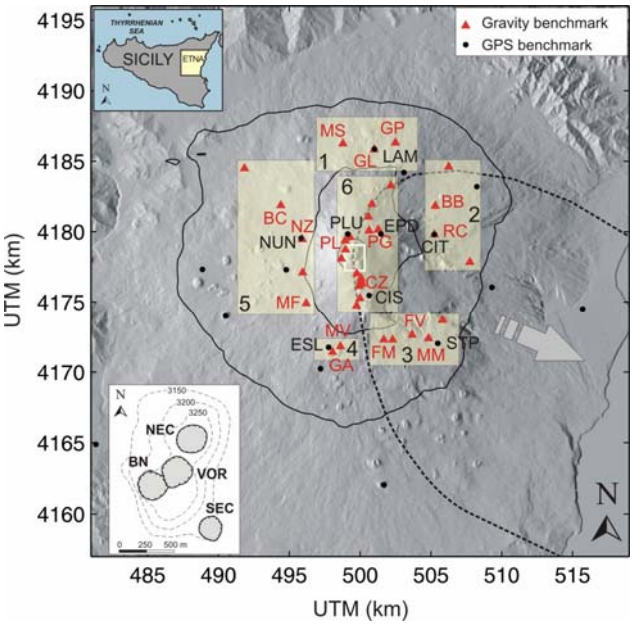

Figure 1

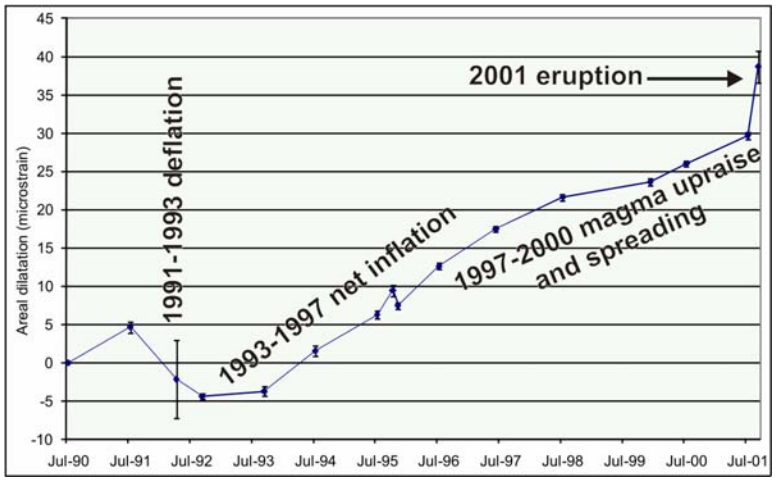

Figure 2

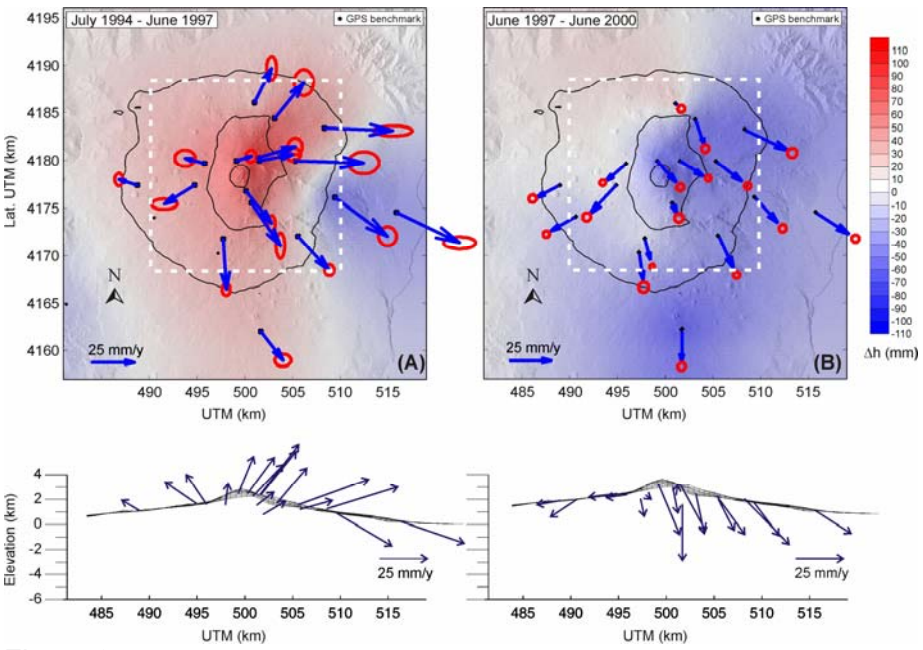

Figure 3

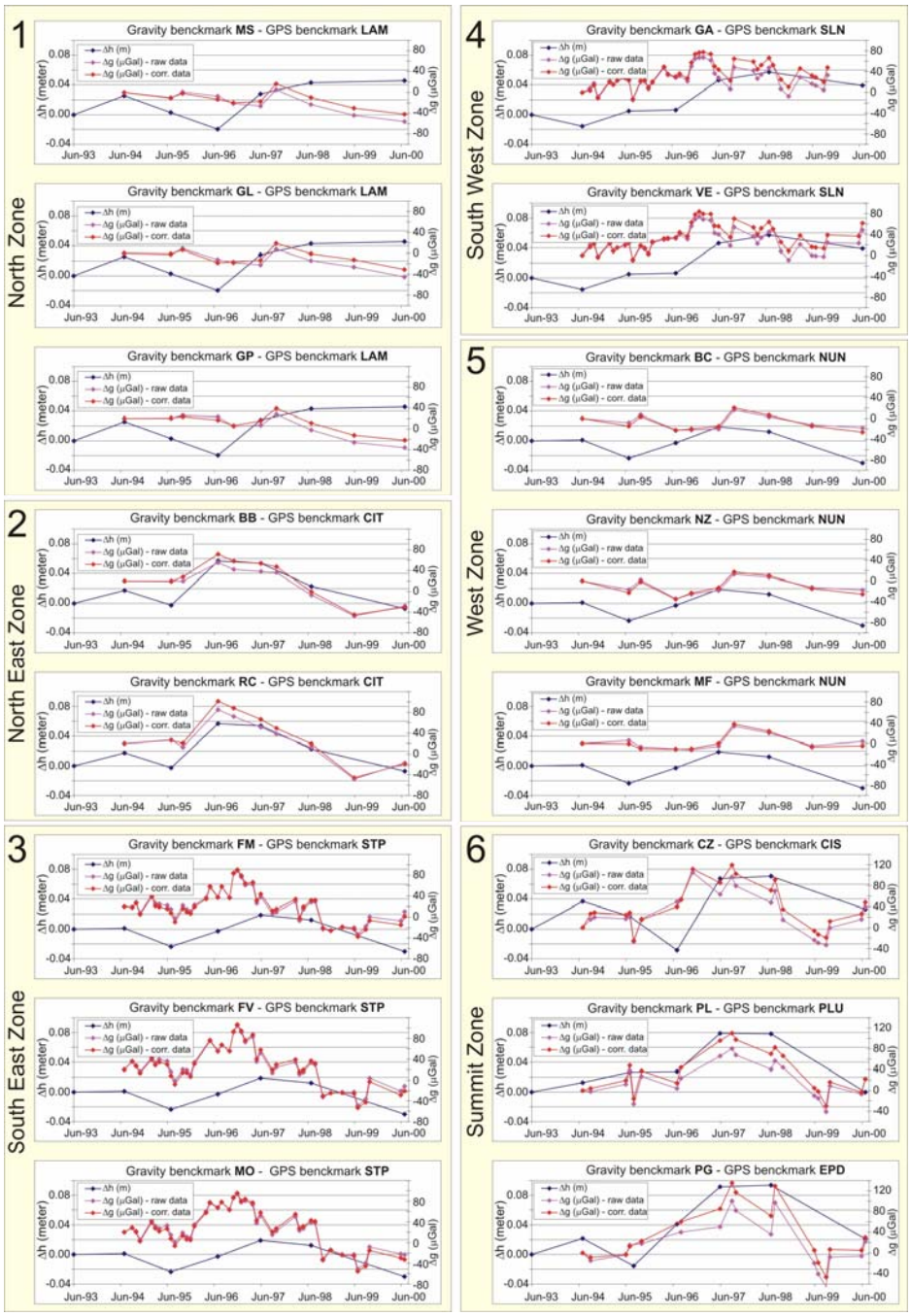

Figure 4

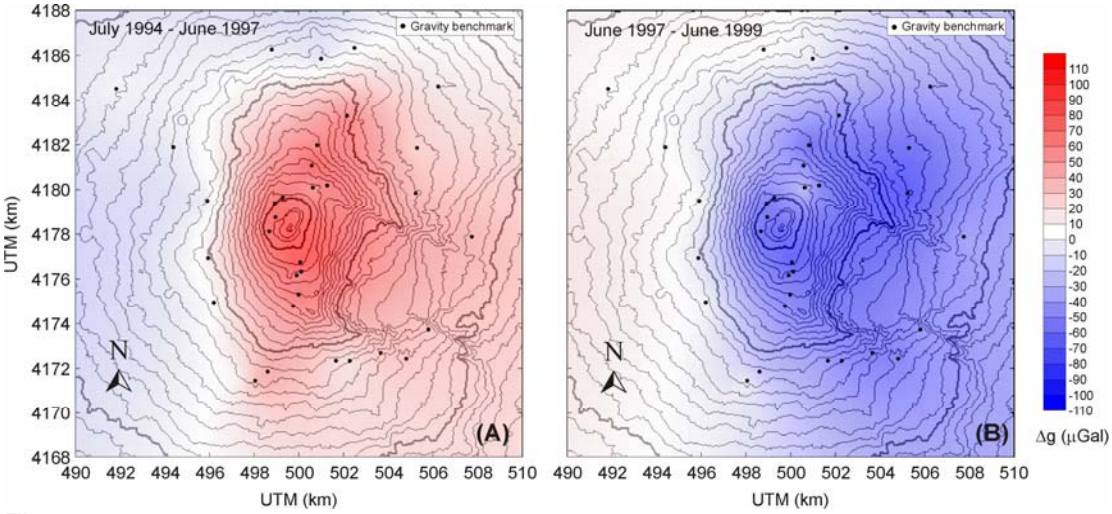

Figure 5

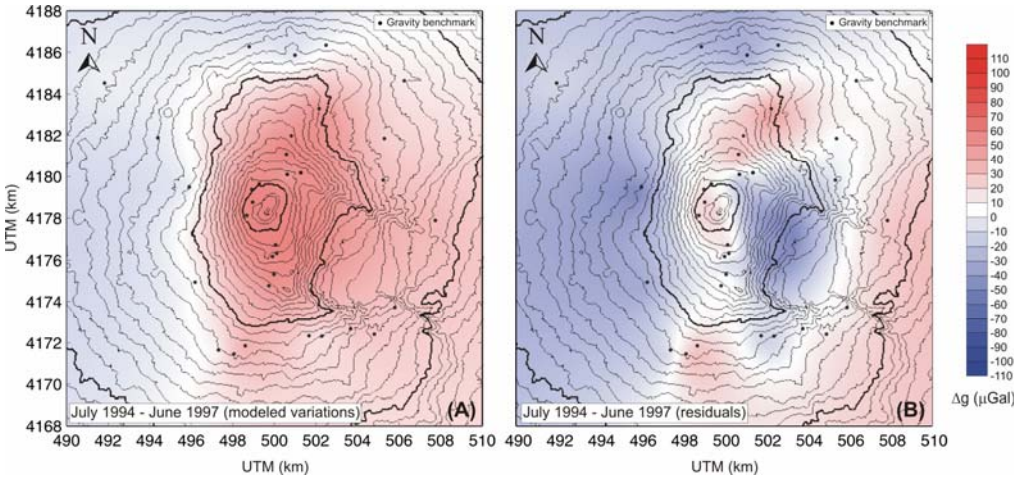

Figure 6

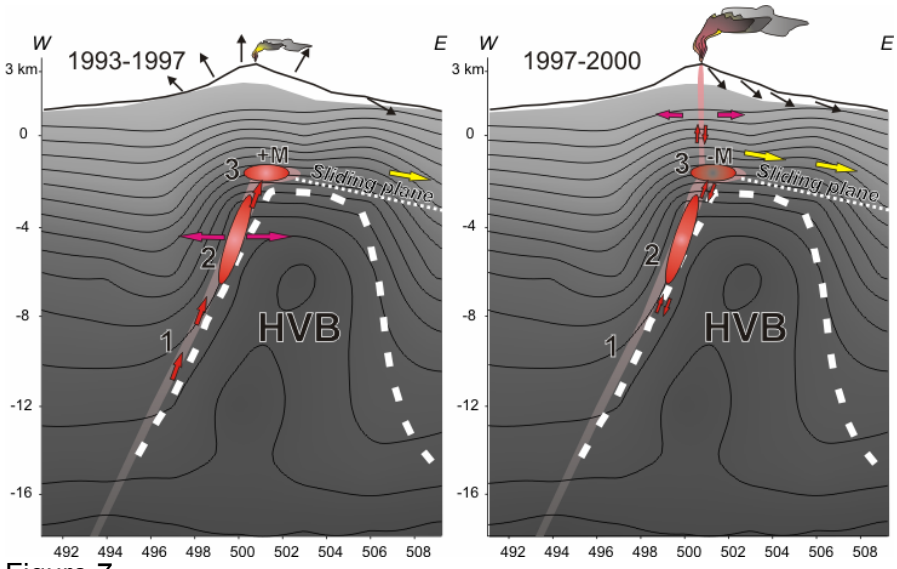

Figure 7

Geometry	Sphere	Prism	Cylinder	Ellipsoid
Xc – Easting (m)	501189	501151	501151	501171
Yc – Northing (m)	4177624	4177805	4177821	4177816
Zc – Center depth (m)	-1820	-2160	-2480	-2300
L - Length (m)		2880		
W – Width (m)		1770	3320	
ϕ - Azimuth (from the North)		-21°		
R - radius (m)			310	
a – semi-major axis (m)				1360
b - semi-minor axis (m)				300
1994-1997				
U* $\Delta\rho$ – thickness* density (kg/m^2)		$6.4*10^4$		
$\Delta\rho$ - density (kg/m^3)			350	390
ΔM - mass change (kg)	$3.2*10^{11}$	$3.4*10^{11}$	$3.5*10^{11}$	$3.5*10^{11}$
Misfit (μGal)	19.37	18.95	19.04	18.99
1997-1999				
U* $\Delta\rho$ – thickness* density (kg/m^2)		$-7.23*10^4$		
$\Delta\rho$ - density (kg/m^3)			-360	-320
ΔM - mass change (kg)	$-3.5*10^{11}$	$-3.7*10^{11}$	$-3.6*10^{11}$	$3.8*10^{11}$
Misfit (μGal)	26.71	25.74	25.86	25.85

Table 1

Period	Activity	**Volume** (x10^6 m^3)
1995-97	Strombolian activity and paroxysmal episodes, lava overflows	7
1998	Strong explosive activity, lava fountains, lava overflow	8
1999 (Feb-Nov)	Summit effusive eruption	25
1999 (Jun-Oct)	Strong explosive activity, several episodes of lava fountains, extensive lava flows	20
2000	66 fire paroxysmal eruptive episodes with lava fountains and extensive lava flows	47
2001 (Jan-Jul)	Strombolian activity, 16 paroxysmal eruptive episodes with extensive lava flows	12
2001 (Jul-Aug)	Flank eruption – effusive and explosive activity	40
2002-03	Flank eruption – effusive and explosive activity	52

Table 2